MEMOIRS OF THE COLLEGE OF SCIENCE UNIVERSITY OF KYOTO, SERIES B,
Vol. XX, No. 4, Article 2, 1953.

The Crystal Structure of Monazite ($CePO_4$)

By

Tateo UEDA

Geological and Mineralogical Institute, University of Kyoto

(Received July 31, 1953)

Abstract

The specimens used in this experiment were found at Ishikawayama, Fukushima Prefecture, Japan. Lattice constants, numbers of chemical unit per unit cell and space group were determined by means of X-ray rotation photographs as well as oscillation photographs. Parameters of atoms were determined through the procedure of *Fourier* syntheses. Results obtained are as follows:

$$a_0 = 6.77 \pm 0.01 \text{ Å}$$
$$b_0 = 6.99 \pm 0.01 \text{ Å}$$
$$c_0 = 6.45 \pm 0.01 \text{ Å}$$
$$\beta = 103^\circ 38' \pm 12'$$
$$V = 297 \text{ Å}^3$$
$$Z = 4$$

space group: $C_{2h}^5 - P2_1/n$

Atoms are in general positions:

$$\pm (xyz;\ 1/2-x,\ 1/2+y,\ 1/2-z).$$

Their parameters are as follows:

	θ_I°	θ_{II}°	θ_{III}°	x	y	z
Ce	81	53	144	0.225	0.147	0.400
P	74	62	−38	0.206	0.172	−0.106
O_I	120	5	26	0.333	0.014	0.072
O_{II}	7	46	−115	0.019	0.128	−0.319
O_{III}	133	90	−84	0.369	0.250	−0.233
O_{IV}	43	115	15	0.119	0.319	0.042

Introduction

Up to the present time, several authors have determined lattice constants, numbers of chemical unit per unit cell and space group of monazite: S. von Gliszczynski[1], in 1939, with the mineral found in Perdatsch, Switzerland; W.

Parrish[2], in the same year, found in Llallagua, Bolivia and Rose C. L. Mooney[3], in 1948, with artificial monazite. Results obtained by these authors are in agreement. C. L. Mooney determined moreover parameters of atoms, though in a preliminary fashion. The parameters, however, involve some discrepancies as pointed out in *Structure Reports*.* It is said that M. P. Kokkoros, in 1942, studying on the crystal structure of this mineral, determined parameters of atoms. The paper, unfortunately, has not been accessible to the writer. A. Pabst[4], however, has related in his paper that Kokkoros's parameters were not in agreement with Mooney's.

Recently, the writer has been employed in X-ray crystallographical studies on monazite which was found at Ishikawayama, Fukushima Prefecture, Japan. The writer will briefly report in the present paper on the lattice constants, numbers of chemical unit, space group and also parameters of atoms of this mineral.

Experiments

Preceding to the X-ray crystallographical investigation, chemical analysis has been carried out. The result is shown in Table 1.

Table 1. (sample, 0.5784 g.)

$[Ce,Y]_2O_3$	P_2O_5	ThO_2	SiO_2	MnO	CaO	MgO	Fe_2O_3	Al_2O_3	$H_2O^{(+)}$	$H_2O^{(-)}$	Total
55.41	26.69	11.73	2.73	—	1.11	—	1.49	0.09	0.05	0.15	99.45

This specimen has also considerable amount of *Th* and *Si* as usually seen in other specimens which were reported by many investigators. To obtain a precise value as possible, measurements of specific gravity were carried out with method proposed by Yoshida and Takei[5] in 1932. Specific gravity of the three specimens, measured one by one, is on the average 5.195. In X-ray photographing, Shearer tube was used installing copper anticathode, and in any case, it was carried out under the condition of 50 kV. and 5 mA. Lattice constants obtained by rotation photographs using *Cu*-K_α radiation ($\lambda = 1.542$ Å) are as follows:

$$a_0 = 6.77 \pm 0.01 \text{ Å}$$
$$b_0 = 6.99 \pm 0.01 \text{ Å}$$
$$c_0 = 6.45 \pm 0.01 \text{ Å}$$
$$\beta = 103^\circ\ 38' \pm 12'$$

Consequently, lattice volume V and numbers of chemical unit in a unit cell Z are as follows respectively:

* Structure Reports, for 1947–1948, vol. 11 (1951).

$$V = 297 \text{ Å}^3$$
$$Z = 3.96 \fallingdotseq 4.$$

The results are in good agreement with those reported by previous investigators. A ratio of $a_0 : b_0 : c_0 = 0.969 : 1 : 0.923$ as well as $103^\circ 38'$ for β angle obtained X-ray photographically are also in good agreement with axial ratio viz. 0.9693 : 1 : 0.9256 and axisl angle viz. $103^\circ 40'$ respectively.*

Oscillation photographs were taken every 10°, oscillating in a rang of 14°, rotating around b axis and also c axis. The regularity of X-ray spectra indicates that space group of this mineral is C_{2h}^5—$P2_1/n$, since reflections $h0l$ and $0k0$ are absent respectively when $h+l$ and k are odd, whereas general reflections show no regularity in absences. The space group is also in agreement with that reported by previous investigators.

Structure Analysis

Intensities of spectra obtained by oscillation photographs were estimated visually, and specified as vvs (very, very strong), vs (very strong), s (strong), m (medium), w (weak), vw (very weak). Besides these, not a few spectra were specified as s^+, m^+, w^+, which mean to be a little stronger than s, m, w respectively. Intensities, observed, of $h0l$ and $hk0$ reflections are shown at the 2nd column in Table 2 and 3 respectively.

In the space group C_{2h}^5—$P2_1/n$, equivalent positions are as follows:

(a) (0 0 0; 1/2 1/2 1/2) (b) (0 0 1/2; 1/2 1/2 0)
(c) (1/2 0 0; 0 1/2 1/2) (d) (1/2 0 1/2; 0 1/2 0)
(e) xyz; $\bar{x}$, 1/2+y, 1/2−z; 1/2−x, −y, z−1/2.

Unit cell contains 4 chemical units of $CePO_4$ as obtained experimentaly, so that $4Ce$, $4P$, $16O$ atoms are present in a unit cell. Then, Ce and P atoms may be situated in the special positions, choosing any two sets out of them. Special positions, however, are included in general ones. Therefore, analysis was carried on assuming that atoms of any kind are situated in general positions.

Rate of intensity, I, of diffraction X-ray which yields equatorial spectrum is expressed as follows:

$$I \propto \left| \pm F \right|^2 \left(\frac{1+\cos^2 2\theta}{\sin 2\theta} \right).$$

Values, $\frac{1+\cos^2 2\theta}{\sin 2\theta}$, for $h0l$ and $hk0$ reflections calculated based on observed glancing angles, θ, are shown at the 4th column in Table 2 and 3 respectively. In space group C_{2h}^5 — $P2_1/n$, structure factor, F_{hkl}, runs:

* Dana's System of Mineralogy, 7th edition, Vol. 1 (1946).

Table 2

$h0l$	I	θ	$\frac{1+\cos^2 2\theta}{\sin 2\theta}$	$\frac{\sin\theta}{\lambda}$
200	vvs	13°33′	3.935	0.15
400	vs	27°57′	1.587	0.30
600	w+	44°43′	1.000	0.46
800	vw (α_1)	69°44′	2.427	0.61
101	vvs	10°53′	5.023	0.12
301	vs	23°31′	2.001	0.26
501	s+	38°48′	1.071	0.41
701	s	59° 1′	1.383	0.56
002	s	14°15′	3.714	0.16
202	—	22°12′	2.159	0.24
402	m+	35°22′	1.175	0.38
602	s	52°59′	1.119	0.52
103	vs	24°23′	1.907	0.27
303	m	34°27′	1.211	0.37
503	w	49°45′	1.041	0.49
004	vs	29°28′	1.446	0.32
204	vs	36°16′	1.143	0.38
404	s+	49° 2′	1.030	0.49
604	s (α_1)	71°20′	2.691	0.62
105	—	40°41′	1.034	0.42
305	vw	51° 4′	1.068	0.50
505	m (α_1)	70°52′	2.610	0.61
006	s	47°35′	1.012	0.48
206	m	55°33′	1.211	0.53
406	—	74°24′	3.343	0.62
107	m+(α_1)	63°37′	1.716	0.58
$10\bar{1}$	vs	8° 33′	6.509	0.10
$30\bar{1}$	m	20° 7′	2.451	0.22
$50\bar{1}$	vw	34°45′	1.198	0.37
$70\bar{1}$	vw	53° 8′	1.123	0.52
$20\bar{2}$	vvs	17°17′	2.958	0.19
$40\bar{2}$	vs	28°23′	1.555	0.31
$60\bar{2}$	vs	43°26′	1.002	0.45
$80\bar{2}$	s (α_1)	65°28′	1.892	0.59
$10\bar{3}$	vvs	21° 6′	2.306	0.23
$30\bar{3}$	s	26°28′	1.708	0.29
$50\bar{3}$	m	37°55′	1.093	0.40
$70\bar{3}$	m	54°47′	1.180	0.53

Table 2 (continued)

$h0l$	I	θ	$\frac{1+\cos^2 2\theta}{\sin 2\theta}$	$\frac{\sin\theta}{\lambda}$
$20\bar{4}$	m^+	29°31′	1.475	0.32
$40\bar{4}$	w	36°25′	1.122	0.39
$60\bar{4}$	vw	49°10′	1.499	0.49
$80\bar{4}$	m (α_1)	71°49′	2.780	0.62
$10\bar{5}$	—	36°43′	1.128	0.39
$30\bar{5}$	w	39°14′	1.061	0.41
$50\bar{5}$	w	48° 1′	1.017	0.48
$70\bar{5}$	m (α_1)	64°21′	1.782	0.59
$20\bar{6}$	vs	46° 1′	1.002	0.47
$40\bar{6}$	s	50°55′	1.065	0.50
$60\bar{6}$	s (α_1)	62°54′	1.655	0.58
$10\bar{7}$	m	57°16′	1.289	0.55
$30\bar{7}$	w^+	58°13′	1.338	0.55
$50\bar{7}$	m (α_1)	67° 1′	2.063	0.60
208	—	73° 4′	3.031	0.62

Table 3

$hk0$	I	θ	$\frac{1+\cos^2 2\theta}{\sin 2\theta}$	$\frac{\sin\theta}{\lambda}$
110	w	9°16′	5.973	0.10
210	s	15° 1′	3.495	0.17
310	w	21°37′	2.235	0.24
410	m^+	28°47′	1.526	0.31
510	m	36°34′	1.133	0.39
610	m^+	45°26′	1.001	0.46
710	m^+	55°52′	1.324	0.54
810	s (α_1)	70°38′	2.571	0.61
020	vs	12°45′	4.215	0.14
120	vvs	14°28′	3.650	0.16
220	w^+	18°47′	2.670	0.21
320	vs	24°32′	1.892	0.27
420	w	31° 9′	1.373	0.34
520	m^+	38°48′	1.071	0.41
620	vw	47°27′	1.011	0.48
720	w	58°13′	1.338	0.55
820	vw (α_1)	74°23′	3.339	0.62
130	w^+	20°33′	2.385	0.23
230	w	23°55′	1.957	0.26

Table 3 (continued)

$hk0$	I	θ	$\frac{1+\cos^2 2\theta}{\sin 2\theta}$	$\frac{\sin\theta}{\lambda}$
330	m$^+$	28°52′	1.520	0.31
430	vw	35° 4′	1.186	0.37
530	s$^+$	42°17′	1.014	0.44
630	vw	51° 4′	1.068	0.50
730	s (α_1)	62° 2′	1.586	0.57
040	vs	26°11′	1.734	0.29
140	s	27°10′	1.649	0.30
240	s$^+$	29°58′	1.446	0.32
340	m$^+$	34°18′	1.217	0.37
440	m$^+$	40° 7′	1.044	0.42
540	w	47° 9′	1.008	0.48
640	w	56°10′	1.237	0.54
740	—	68°39′	2.271	0.60
150	—	34°18′	1.217	0.37
250	m	36°52′	1.123	0.39
350	—	40°50′	1.032	0.42
450	m$^+$	46°26′	1.004	0.47
550	—	53°35′	1.138	0.52
650	m$^+$(α_1)	63°16′	1.686	0.58
060	s	41°25′	1.024	0.43
160	m	42°17′	1.014	0.44
260	m$^+$	44°34′	1.000	0.46
360	w	48°36′	1.024	0.49
460	m	54°11′	1.158	0.53
560	w$^+$(α_1)	62° 2′	1.586	0.57
660	w$^+$(α_1)	74°40′	3.411	0.63
170	—	51°21′	1.075	0.51
270	—	53°44′	1.143	0.52
370	vw	58° 4′	1.330	0.55
470	w (α_1)	64°32′	1.800	0.59
570	s (α_1)	75°32′	3.650	0.63
080	w (α_1)	61°52′	1.573	0.57
180	s (α_1)	62°43′	1.640	0.58
280	w (α_1)	65°50′	1.930	0.59
380	s (α_1)	71°34′	2.733	0.62

$$F_{hkl}=\Sigma\, 4 f_{\circ} \cos 2\pi\ (hx+lz+\frac{h+k+l}{4}) \cos 2\pi\ (ky-\frac{h+k+l}{4}),$$

Therefore,

$$F_{h0l}=\Sigma\, 4\, f_{\circ}\cos\left\{h\,\theta_{\mathrm{I}}+l\,\theta_{\mathrm{III}}+\frac{\pi\,(h+l)}{2}\right\}\cos\left\{-\frac{\pi\,(h+l)}{2}\right\}$$

$$F_{hk0}=\Sigma\, 4\, f_{\circ}\cos\left\{h\,\theta_{\mathrm{I}}+\frac{\pi\,(h+k)}{2}\right\}\cos\left\{k\,\theta_{\mathrm{II}}-\frac{\pi\,(h+k)}{2}\right\}$$

where, $f_{\circ}$ is an atomic scattering factor, which is a function of $\frac{\sin\theta}{\lambda}$. At the 5th column in Table 2 and 3, values, $\frac{\sin\theta}{\lambda}$, for *h0l* and *hk0* reflections are given respectively, where values, θ, are observed glancing angles and λ is 1.542 Å (Cu-K_{α}) or 1.540 Å (Cu-K_{α_1}). For $f_{\circ}$, Hartree's values corresponding $\frac{\sin\theta}{\lambda}$ were used.

Atomic numbers of *Ce*, *P* and *O* atoms are 58, 15 and 8 respectively; so that it is considered that the position of *Ce* atom in a lattice should exert a great influence on the intensities of reflections. Then, approximate $\theta_{\mathrm{I}}^{\circ}$ and $\theta_{\mathrm{III}}^{\circ}$ parameters for *Ce* atom may be found through the intensities of reflections of *h00*, *00l* and several *h0l* reflections. Approximate $\theta_{\mathrm{I}}^{\circ}$ and $\theta_{\mathrm{II}}^{\circ}$ parameters for *Ce* atom may also be found through the intensities of reflections of *h00*, *0k0* and several *hk0* reflections. The intensities, calculated, of 200, 400, 600 and 800 reflections corresponding θ_{I}^{e} for *Ce* atom are illustrated in Fig. I. Whereas, the intensities,

Fig. I. The intensity curves of *h00* corresponding $\theta_{\mathrm{I}}^{\circ}$ for *Ce* atom alone.
(The same curves repeat every 90°)

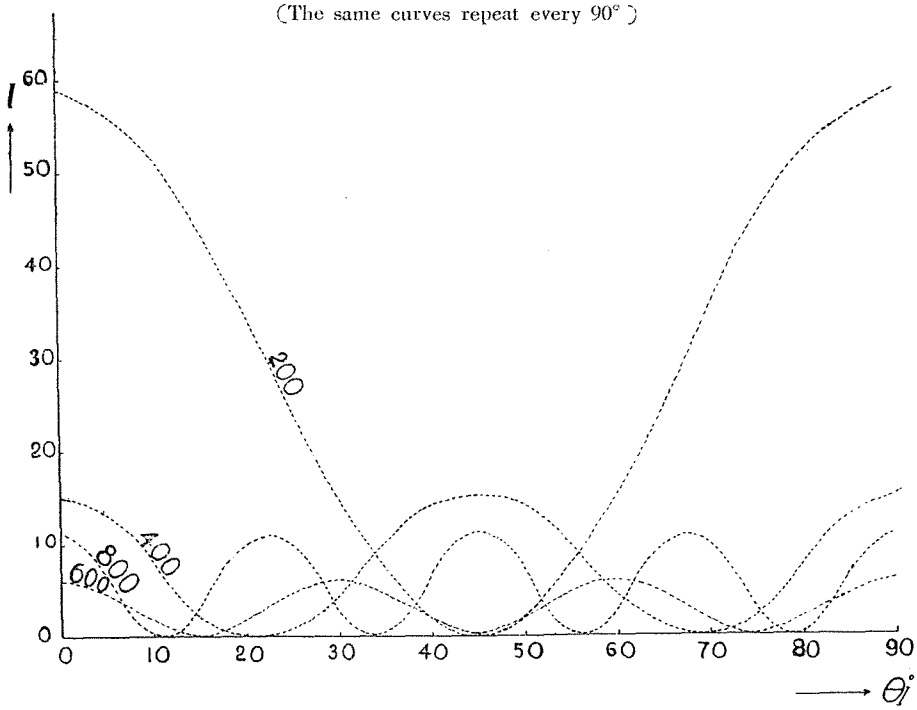

observed, of 200, 400, 600 and 800 reflections are vvs, vs, w^+ and $vw(\alpha_1)$ respectively; hence, θ_I° for *Ce* atom must be any one of ~9°~, ~81°~, ~99°~, ~171°~, ~189°~, ~261°~, ~279°~, ~351°~ (notation of ~9°~ means the neighbourhood of 9°, and the same is applied to the rest). The intensities, calculated, of 002, 004 and 006 reflections corresponding θ_{III}° for *Ce* atom are illustrated in Fig. II.

Fig. II. The intensity curves of *00l* corresponding θ_{III}° for *Ce* atom alone. (The same curves repeat every 90°)

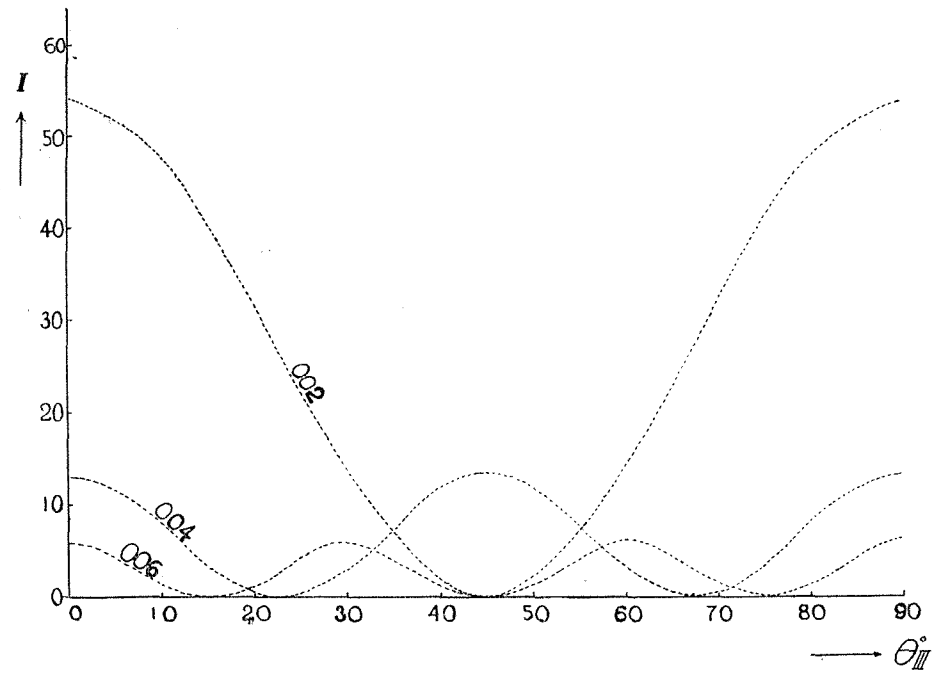

The intensities, observed, of 002, 004 and 006 are s, vs and s respectively. Hence, θ_{III}° for *Ce* atom must be any one of ~37°~, ~53°~, ~127°~, ~143°~, ~217°~, ~233°~, ~307°~, ~323°~. Therefore, probable $(\theta_I^\circ, \theta_{III}^\circ)$ for *Ce* atom must be any one of 64 sets combining any of θ_I° with any of θ_{III}°, obtained above respectively. Taking space group of this mineral into account, probable $(\theta_I^\circ, \theta_{III}^\circ)$ for *Ce* atom, however, should be any one of 16 sets combining ~9°~ or ~81°~ for θ_I° with any of θ_{III}°, obtained above.

Using these 16 sets of probable $(\theta_I^\circ, \theta_{III}^\circ)$ for *Ce* atom, the intensities of 301, 501, 404, 602, $40\bar{2}$, $60\bar{2}$, and $60\bar{6}$ reflections are calculated. The results are shown in Table 4. The intensities, observed, of these reflections are vs, s^+, s^+, s, vs, vs and $s(\alpha_1)$ respectively. Hence, as the most probable $(\theta_I^\circ, \theta_{III}^\circ)$ for *Ce* atom, (~9°~, ~127°~), (~9°~, ~307°~), (~81°~, ~143°~), (~81°~, ~323°~) are obtained. However, only the same structures are obtainable from (~9°~, ~127°~) and (~9°~,

~307°~); the same is applied in the case of (~81°~, ~143°~) and (~81°~, ~323°~). Accordingly, only (~9°~, ~127°~) and (~81°~, ~143°~) remain as the most probable ($\theta_{\mathrm{I}}^{\circ}$, $\theta_{\mathrm{III}}^{\circ}$) for *Ce* atom.

The intensities, calculated, of 020, 040, 060 and 080 reflections corresponding $\theta_{\mathrm{II}}^{\circ}$ for *Ce* atom are illustrated in Fig III.

Fig. III. The intensity curves of *0k0* corresponding $\theta_{\mathrm{II}}^{\circ}$ for *Ce* atom alone. (The same curves repeat every 90°)

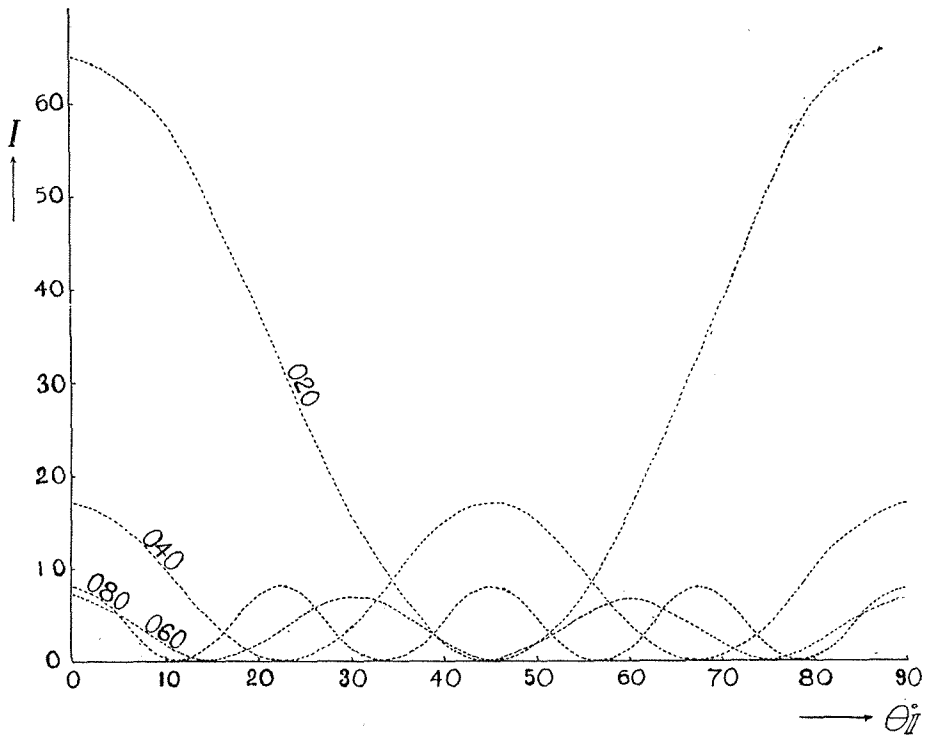

Whereas, the intensities, observed, of 020, 040, 060 and 080 reflections are vs, vs, s and w(α_1) respectively. Hence, $\theta_{\mathrm{II}}^{\circ}$ for *Ce* atom must be any one of ~37°~,~53°~,~127°~,~143°~,~217°~,~233°~,~307°~,~323°~. Consequently, probable ($\theta_{\mathrm{I}}^{\circ}$, $\theta_{\mathrm{II}}^{\circ}$) for *Ce* atom must be any one of 16 sets combining any of these $\theta_{\mathrm{II}}^{\circ}$ with ~9°~ or ~81°~ which are the most probable parameters for $\theta_{\mathrm{I}}^{\circ}$. Using these 16 sets of probable ($\theta_{\mathrm{I}}^{\circ}$, $\theta_{\mathrm{II}}^{\circ}$) for *Ce* atom, the intensities of 120, 320, 530, 240, 570, 180, 380 reflections were calculated. The results are shown in Table 5. The intensities, observed, of these reflections are vvs. vs, s^+, s^+, s(α_1), s(α_1), s(α_1). Hence, as the most probable ($\theta_{\mathrm{I}}^{\circ}$, $\theta_{\mathrm{II}}^{\circ}$) for *Ce* atom, (~81°~, ~53°~),(~81°~,~127°~),(~81°~,~233°~),(~81°~,~307°~) are obtained. From

Table 4

$\theta_{\mathrm{I}}^{\circ}$	$\theta_{\mathrm{III}}^{\circ}$	I_{301}	I_{501}	$I_{\bar{4}04}$	I_{602}	$I_{40\bar{2}}$	$I_{60\bar{2}}$	$I_{60\bar{6}}$
9	37	4.21	0.14	5.83	2.23	9.09	5.58	7.49
9	127	17.75	7.30	5.83	2.23	9.09	5.58	7.49
9	217	4.21	0.14	5.83	2.23	9.09	5.58	7.49
9	307	17.75	7.30	5.83	2.23	9.09	5.58	7.49
9	53	0.67	0.14	0.81	5.25	1.70	2.40	0.09
9	143	21.12	7.30	0.81	5.25	1.70	2.40	0.09
9	233	0.67	0.14	0.81	5.25	1.70	2.40	0.09
9	323	21.12	7.30	0.81	5.25	1.70	2.40	0.09
81	37	0.67	0.14	0.81	5.25	1.70	2.40	0.09
81	127	21.12	7.30	0.81	5.25	1.70	2.40	0.09
81	217	0.67	0.14	0.81	5.25	1.70	2.40	0.09
81	307	21.12	7.30	0.81	5.25	1.70	2.40	0.09
81	53	4.21	0.14	5.83	2.23	9.09	5.58	7.49
81	143	17.75	7.30	5.83	2.23	9.09	5.58	7.49
81	233	4.21	0.14	5.83	2.23	9.09	5.58	7.49
81	323	17.75	7.30	5.83	2.23	9.09	5.58	7.49

Table 5

$\theta_{\mathrm{I}}^{\circ}$	$\theta_{\mathrm{II}}^{\circ}$	I_{120}	I_{320}	I_{530}	I_{240}	I_{570}	I_{180}	I_{380}
9	37	1.23	3.77	0.41	8.59	0.27	0.16	1.98
9	53	1.23	3.77	2.87	8.59	7.48	0.16	1.98
9	127	1.23	3.77	2.87	8.59	7.48	0.16	1.98
9	143	1.23	3.77	0.41	8.59	0.27	0.16	1.98
9	217	1.23	3.77	0.41	8.59	0.27	0.16	1.98
9	233	1.23	3.77	2.87	8.59	7.48	0.16	1.98
9	307	1.23	3.77	2.87	8.59	7.48	0.16	1.98
9	323	1.23	3.77	0.41	8.59	0.27	0.16	1.98
81	37	47.74	14.67	0.41	8.59	0.27	6.01	7.56
81	53	47.74	14.67	2.87	8.59	7.48	6.01	7.56
81	127	47.74	14.67	2.87	8.59	7.48	6.01	7.56
81	143	47.74	14.67	0.41	8.59	0.27	6.01	7.56
81	217	47.74	14.67	0.41	8.59	0.27	6.01	7.56
81	233	47.74	14.67	2.87	8.59	7.48	6.01	7.56
81	307	47.74	14.67	2.87	8.59	7.48	6.01	7.56
81	323	47.74	14.67	0.41	8.59	0.27	6.01	7.56

these 4 sets, however, only the same structures are obtainable. Then, it is sufficient only to take (~81°~, ~53°~) as the most probable ($\theta_{\mathrm{I}}^{\circ}$, $\theta_{\mathrm{II}}^{\circ}$) for *Ce* atom. In consequence, *approximate* parameters for *Ce* atom are determined uniquely: that is (81°, 53°. 143°).

Now; assuming that *O* atoms may pack in a tetrahedron whose edges are about 2.64 Å in length, twice as large as ion radius of O^{2-}, and *P* atom may be situated at the center of this tetrahedron; the parameters of the atoms of every kind were searched for by means of *trial and error*. The results obtained are shown in Table 6.

Table 6

	$\theta_{\mathrm{I}}^{\circ}$	$\theta_{\mathrm{II}}^{\circ}$	$\theta_{\mathrm{III}}^{\circ}$
Ce	81	53	144
P	78	54	-39
O_{I}	133	-4	30
O_{II}	16	31	-114
O_{III}	132	89	-87
O_{IV}	29	96	15

If the values, shown in Table 6, be given respectively as the parameters of the atoms of every kind, the intensities, calculated, of *h0l* and *hk0* reflections are as shown at the 4th column in Table 7 and 8 respectively. When these intensities, calculated, are compared with those observed experimentally, it is comprehensible that both are in considerably good agreement.

Space group C_{2h}^{5}—$P2_1/n$ has centers of inversion. Using structure factors of *h0l* and *hk*0 lattice planes, calculated with parameters obtained by the method of *trial and error*, which are shown at the 3rd column in Table 7 and 8 respectively, two dimensional *Fourier* syntheses were then carried out. Adopting a center of inversion as an origion, electron cloud density, $\rho\,(x,\ z)$ per unit area at a point $(x,\ z)$ projected on xz plane runs:

Table 7

h0l	*I* observed	obtained by *trial and error*		obtained by *Fourier* summation	
		F	*I*	*F*	*I*
200	vvs	-193	54.89	-213	66.77
400	vs	125	9.29	121	8.69
600	w+	-91	3.10	-56	1.17
800	vw (α_1)	37	1.21	33	0.99

Table 7 (continued)

h0l	*I* observed	obtained by *trial and error*		obtained by *Fourier* summation	
		F	*I*	*F*	*I*
101	vvs	−117	25.75	−116	25.28
301	vs	142	15.16	130	12.65
501	s$^+$	−106	4.50	−122	5.96
701	s	88	3.97	99	5.07
002	s	61	5.18	66	6.05
202	—	5	0.02	−8	0.05
402	m$^+$	−80	2.82	−86	3.25
602	s	71	2.09	94	3.70
103	vs	−127	11.52	−131	12.24
303	m	69	2.15	82	3.05
503	w	−50	0.97	−46	0.82
004	vs	−144	11.48	−141	10.75
204	vs	178	13.51	172	12.65
404	s$^+$	−154	9.14	−163	10.23
604	s (α_1)	115	13.11	116	13.54
105	—	3	0.00	−7	0.02
305	vw	−53	1.11	−46	0.85
505	m (α_1)	39	1.44	54	2.85
006	s	−127	6.09	−127	6.10
206	m	69	2.14	73	2.41
406	—	−23	0.65	−16	0.32
107	m$^+$(α_1)	90	5.15	87	4.86
10$\bar{1}$	vs	57	7.92	65	10.29
30$\bar{1}$	m	−41	1.55	−50	2.29
50$\bar{1}$	vw	−20	0.18	−17	0.13
70$\bar{1}$	vw	19	0.15	26	0.28
20$\bar{2}$	vvs	−131	19.00	−152	25.56
40$\bar{2}$	vs	175	17.87	166	16.03
60$\bar{2}$	vs	−146	7.97	−154	8.89
80$\bar{2}$	s (α_1)	133	12.50	119	10.02
10$\bar{3}$	vvs	212	38.83	213	39.13
30$\bar{3}$	s	−84	4.51	−103	6.78
50$\bar{3}$	m	82	2.77	85	2.95
70$\bar{3}$	m	−83	3.01	−73	2.35
20$\bar{4}$	m$^+$	103	5.87	99	5.41
40$\bar{4}$	w	−60	1.53	−52	1.13
60$\bar{4}$	vw	−4	0.01	−27	0.41
80$\bar{4}$	m (α_1)	33	1.13	49	2.50

Table 7 (continued)

h0l	*I* observed	obtained by *trial and error*		obtained by *Fourier* summation	
		F	*I*	*F*	*I*
$10\bar{5}$	—	25	0.26	20	0.17
$30\bar{5}$	w	−50	0.99	−52	1.07
$50\bar{5}$	w	76	2.20	59	1.32
$70\bar{5}$	m (α_1)	−71	3.34	−76	3.85
$20\bar{6}$	vs	165	10.18	171	10.96
$40\bar{6}$	s	−117	5.43	−125	6.22
$60\bar{6}$	s (α_1)	128	10.05	110	7.49
$10\bar{7}$	m	−69	2.28	−65	2.04
$30\bar{7}$	w$^+$	59	1.73	64	2.05
$50\bar{7}$	m (α_1)	−47	1.67	−57	2.51
$20\bar{8}$	–	−6	0.04	−1	0.00

Table 8

hk0	*I* observed	obtained by *trial and error*		obtained by *Fourier* summation	
		F	*I*	*F*	*I*
110	w	26	1.51	21	0.99
210	s	−65	5.56	−66	5.69
310	w	−35	1.03	−23	0.44
410	m$^+$	71	2.89	92	4.83
510	m	84	3.00	79	2.64
610	m$^+$	−118	5.21	−112	4.70
710	m$^+$	−86	3.36	−76	2.86
810	s (α_1)	106	10.62	98	9.23
020	vs	−83	10.86	−96	14.53
120	vvs	−224	68.68	−210	60.20
220	w$^+$	57	3.28	54	2.91
320	vs	164	19.22	167	19.73
420	w	−32	0.53	−27	0.37
520	m$^+$	−116	5.42	−106	4.50
620	vw	30	0.34	26	0.26
720	w	44	0.97	30	0.45
820	vw (α_1)	−6	0.04	−13	0.21
130	w$^+$	−40	1.43	−46	1.89
230	w	−40	1.17	−29	0.62
330	m$^+$	92	4.20	89	4.50
430	vw	38	0.59	23	0.23
530	s$^+$	−105	4.12	−134	6.81

Table 8 (continued)

hk0	*I* observed	obtained by *trial and error*		obtained by *Fourier* summation	
		F	*I*	*F*	*I*
630	vw	-41	1.35	-30	0.36
730	s (α_1)	108	6.92	112	7.44
040	vs	-129	10.79	-139	12.53
140	s	100	6.19	99	6.04
240	s$^+$	149	12.03	114	7.03
340	m$^+$	-93	3.94	-96	4.19
440	m$^+$	-136	7.22	-121	5.71
540	w	43	0.70	59	1.31
640	w	61	1.72	61	1.72
740	—	-33	0.92	-14	0.17
150	—	-26	0.31	-16	0.12
250	m	52	1.14	79	2.62
350	—	7	0.02	0	0.00
450	m$^+$	-106	4.22	-94	3.32
550	—	0	0.00	7	0.02
650	m$^+$(α_1)	104	6.82	100	6.31
060	s	103	4.07	135	6.98
160	m	108	4.42	81	2.49
260	m$^+$	-121	5.48	-115	4.95
360	w	-78	2.33	-62	1.47
460	m	85	3.13	80	2.77
560	w$^+$(α_1)	63	2.35	58	2.00
660	w$^+$(α_1)	-46	2.70	-40	2.04
170	—	18	0.13	24	0.23
270	—	14	0.08	-31	0.41
370	vw	-65	2.09	-45	1.01
470	vw (α_1)	28	0.53	31	0.65
570	s (α_1)	90	11.06	81	8.96
080	w (α_1)	73	3.11	47	1.30
180	s (α_1)	118	8.51	-118	8.54
280	vw (α_1)	-53	2.03	-29	0.61
380	s (α_1)	-105	11.10	97	9.62

$$\rho\ (x,\ z)=\frac{1}{a_o c_o \sin\beta}\times\sum_{-\infty}^{\infty}\sum_{-\infty}^{\infty}\left|F(h0l)\right|\cos\left\{h\cdot 2\pi x+l\cdot 2\pi z-\alpha(h0l)\right\},$$

and electron cloud density, $\rho\ (x,\ y)$ runs:

$$\rho\ (x,y)=\frac{1}{a_o b_o}\times\sum_{-\infty}^{\infty}\sum_{-\infty}^{\infty}\left|F\ (hk0)\right|\cos\left\{h\cdot 2\pi x+k\ 2\pi y-\alpha\ (hk0)\right\}.$$

Fig. IV. Electron cloud density curve projected on xz plane.

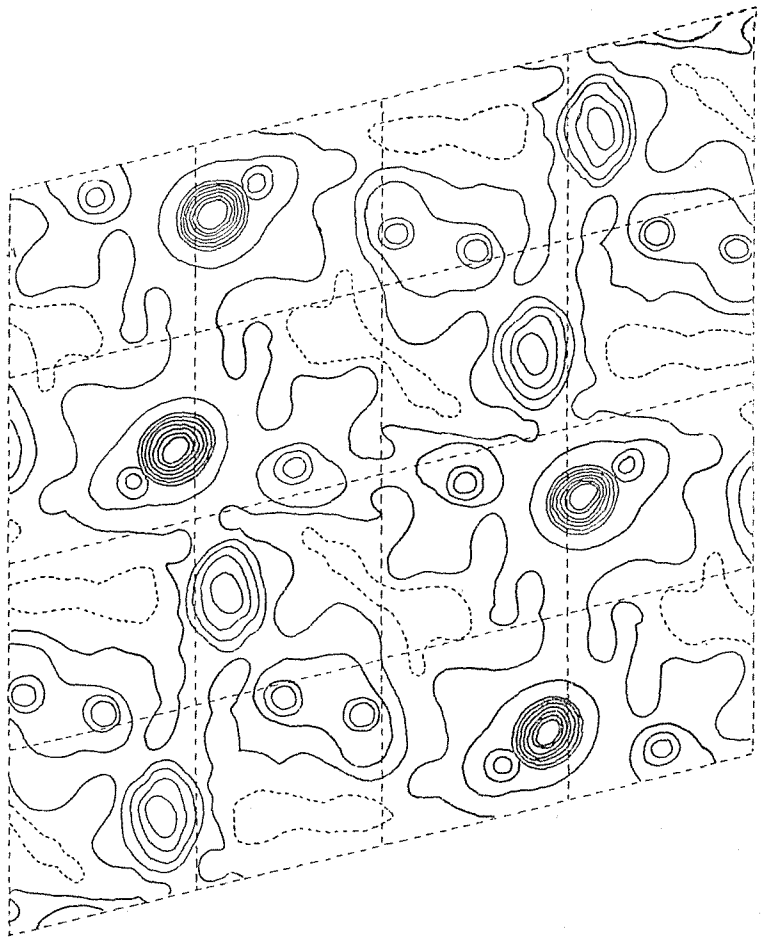

Table 9

	$\theta_{\mathrm{I}}^{\circ}$	$\theta_{\mathrm{II}}^{\circ}$	$\theta_{\mathrm{III}}^{\circ}$	x	y	z
Ce	81	53	144	0.225	0.147	0.400
P	74	62	−38	0.206	0.172	−0.106
O_{I}	120	5	26	0.333	0.014	0.072
O_{II}	7	46	−115	0.019	0.128	−0.319
O_{III}	133	90	−84	0.369	0.250	−0.233
O_{IV}	43	115	15	0.119	0.319	0.042

Fig. V. Electron cloud density curve projected on *xy* plane.

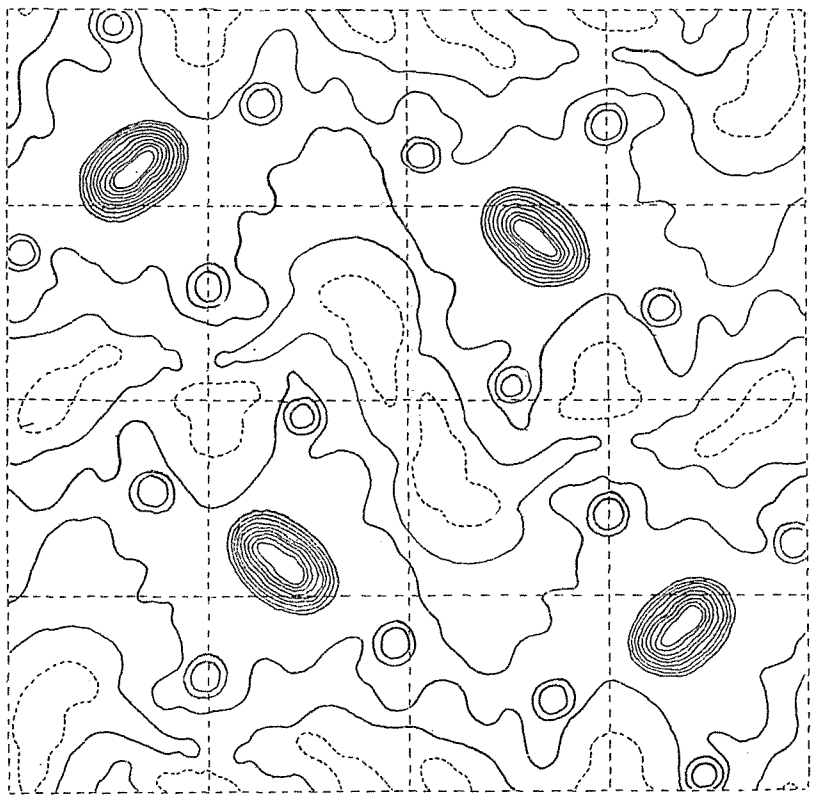

The summation was, at any case, carried out on four hundreds points in one fourth of area of projections and was repeated several times with structure factors obtained by preceding summation. Electron cloud density curves projected on *xz* and *xy* planes obtained finally by *Fourier* syntheses are shown in Fig. IV and V respectively.

Parameters of the atoms of every kind, obtained after several times repetitions of *Fourier* syntheses are shown in Table 9.

These parameters now obtained are not in agreement with those reported by Rose C. L. Mooney[6].

Basing on these parameters, structure factors of *h0l* and *hk0* lattice planes and intensities of *h0l* and *hk0* reflections are calculated which are shown at the 5th and the 6th column in Table 7 and 8 respectively.

Comparing these intensities calculated above with those observed experimentally, it is comprehensible that both are in good agreement. In Fig. VI and VII, the crystal structure of this mineral projected on *xz* and *xy* planes is illustrated respectively.

Fig. VI. The crystal structure of monazite projected on xz plane.

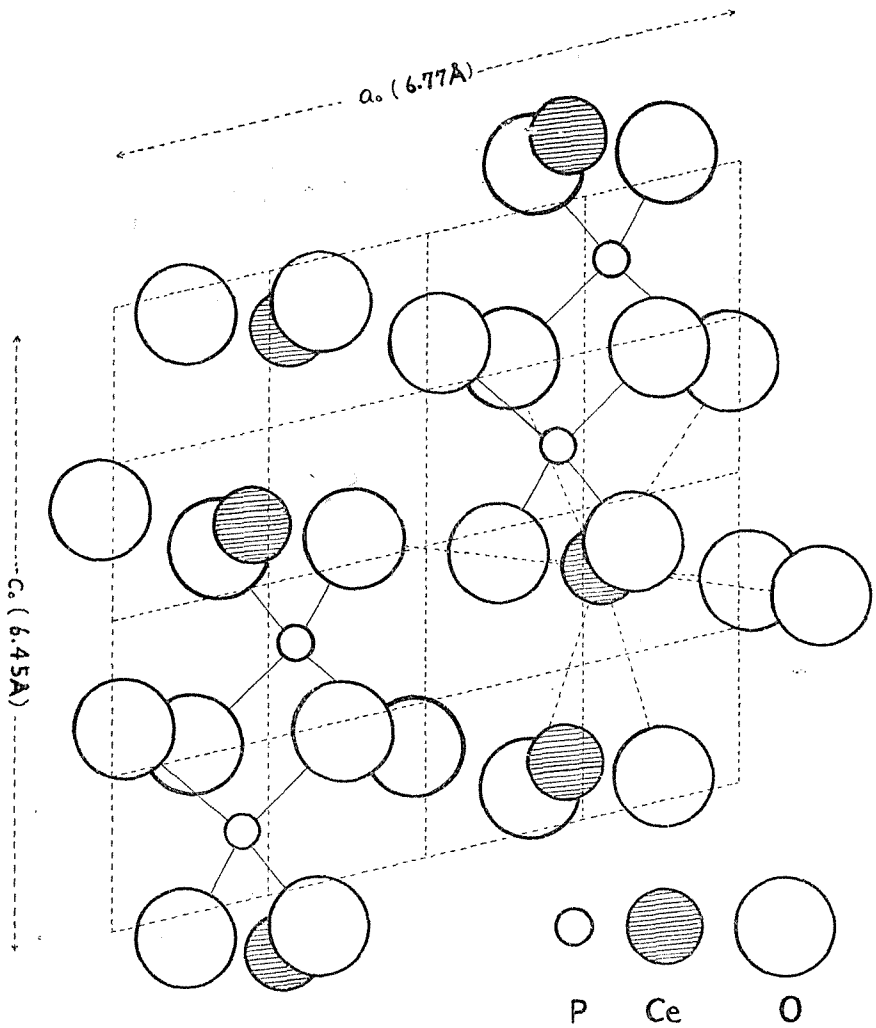

Structure Description

In this structure, P atom is situated at the center of a more or less deformed tetrahedron of four O atoms, where O–P distances are 1.66 Å, 1.66 Å, 1.62 Å, 1.62 Å respectively. They are 1.64 Å on the average. Provided that ion radii of O^{2-} and P^{5+} are 1.32 Å and 0.34 Å respectively, the average distance 1.64 Å, obtained experimentally as a distance of O–P, is a little smaller than the sum of these two ion radii 1.66 Å. O–O distances belonging to the same tetrahedron

Fig. VII. The crystal structure of monazite projected on xy plane.

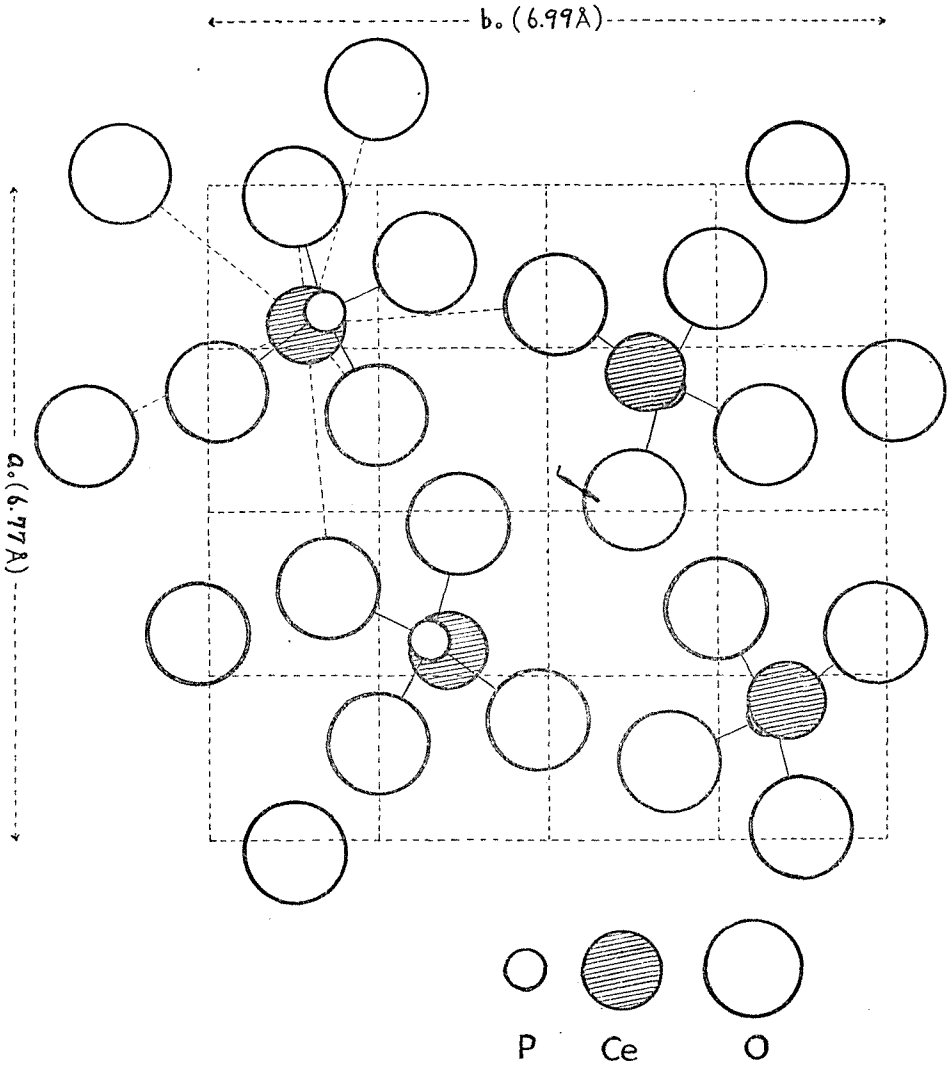

are 2.96 Å, 2.77 Å, 2.68 Å, 2.62 Å, 2.57 Å, 2.43 Å respectively. They are 2.67 Å on the average, which is a little larger than the twice of the radius of O^{2-}. O–O distances which belong to another tetrahedron, are not less than 2.47 Å. Ce atom is surrounded by nine O atoms which form irregular polyhedron. O–Ce distances are 2.63 Å, 2.60 Å, 2.60 Å, 2.54 Å, 2.54 Å, 2.50 Å, 2.50 Å, 2.43 Å, 2.43 Å respectively. Then they are 2.53 Å on the average. Taking the radius of Ce^{3+} to be 1.18 Å, sum of the radii of O^{2-} and Ce^{3+} amounts to

2.50 Å. The average distance 2.53 Å obtained experimentally as a distance of *O–Ce*, is a little larger than the sum of these two ion raddi 2.50 Å.

O atom is shared by one *P* atom and two *Ce* atoms. The strength of electrostatic bonding between *O* atom and *P* atom is 5/4, and that between *O* atom and *Ce* atom is 3/9. Total sum of the strength of electrostatic bonding is 23/12, which is nearly equal to 2, and that is the charge of *O* atom. Hence, Pauling's principle is in this structure satisfied.

Monazite crystal has a distinct cleavage parallel to (100). If we take the arrangement of PO_4 atoms groups into account, this character will be immediately recognized.

Discussion

It is well known that minerals bearing radio active elements are, more or less, in a state of metamict, with several exceptions such as xenotime, monazite, titanite and thortveitite. With regard to the cause which gives rise to metamictization, many authors have hitherto given their opinions.

F. Machatschki[7] has offered his opinion with regared to this phenomenon, that the constant bombardment of α–particle, accompanied by disintegration of radio active elements, is not solely the cause of metamictization, the crystal must *apriori* be instable structurally.

In the structure of zircon, which is sometimes found in a state of metamict, *Zr* atom is eight-coordination accordiug to L. Vegard[8], O. Hassel[9], W. Binks[10], R. W. G. Wyckoff and S. B. Hendricks[11], although it is postulated to be six- or seven-coordination, since radius ratio of Zr^{4+} to O^{2-} is about 0.659. The irregularity of *Zr–O* distances, that is four *O* atoms at 2.05 Å and four at 2.41 Å, may probably be due to this forced coordination. In the structure of xenotime, *Y* atom is eight-coordination according to L. Vegard[12]. It is naturally postulated to be eight-coordination, since radius ratio of Y^{3+} to O^{2-} is about 0.803.

In the structure of monazite, *Ce* atom is postulated to be more than eight-, or probably nine-coordination, since radius ratio of Ce^{3+} to O^{2-} is about 0.894. This postulation is actually satified in this structure. Relation between radius ratio and coordination number is satisfied in the structure of titanite as well as thortveitite. If huttonite have the same structure as that of monazite, A. Pabst[13] is of this opinion, the relation under consideration is satisfied.

F. Machatschki[14] has not made clear what *structural instability* means. The writer is of the opinion that structual instability may be explained from the standpoint of discrepancy between radius ratio and coordination number.

Acknowledgment

The writer wishes to express his cordial thanks to Dr. J. Takubo, Professor of Kyoto University and to Dr. R. Kiriyama, assistant Professor of Osaka University, who gave him kind advices in this study.

This research work has been made possible by the fund of Hattori Hoko-Kai, and for their generosity the writer also wishes to express his sincere gratitude.

Literatures

1 GLISZCZYNSKI, S. von: Z. f. Krist., 101, 1 (1939).
2 PARRISH, W.: Am. Miner., 24, 651 (1939).
3 MOONEY, Rose C. L.: J. Chem. Phys., 16, 1003 (1948).
4 PABST, A.: Am. Miner., 36, 60 (1951).
5 YOSHIDA, U. and TAKEI, B.: Memoirs of Coll. of Sci., Kyoto Imp. Univ., A, 15, 1 (1932).
6 Loc. cit.
7 MACHATSCHKI, F.: Zentralblatt Miner., Abt. A, 38 (1941).
8 VEGARD, L.: Phil. Mag., 1, 1151 (1926).
9 HASSEL, O.: Zeit. f. Krist., 63, 247 (1926).
10 BINKS, W.: Miner. Mag., 21, 176 (1926).
11 WYCKOFF, R. W. G. and HENDRICKS, S. B.: Zeit. f. Krist., 66, 73 (1927).
12 VEGARD, L.: Phil. Mag., 4, 511 (1927).
13 Loc. cit.
14 Loc. cit.